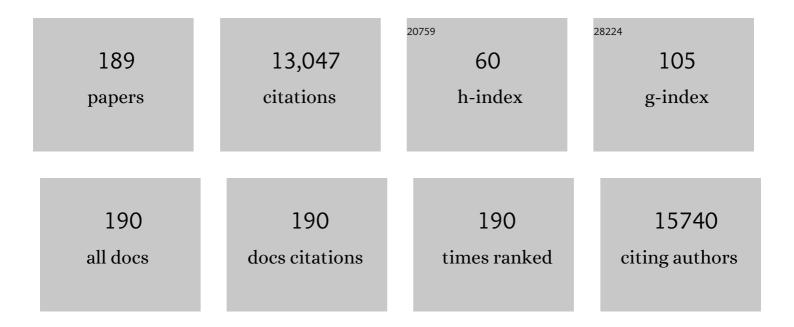
Jianlong Wang

List of Publications by Year in descending order

Source: https://exaly.com/author-pdf/3774474/publications.pdf Version: 2024-02-01



#	Article	IF	CITATIONS
1	An Extended Transcriptional Network for Pluripotency of Embryonic Stem Cells. Cell, 2008, 132, 1049-1061.	13.5	1,226
2	A protein interaction network for pluripotency of embryonic stem cells. Nature, 2006, 444, 364-368.	13.7	1,003
3	Nickel sulfide microsphere film on Ni foam as an efficient bifunctional electrocatalyst for overall water splitting. Chemical Communications, 2016, 52, 1486-1489.	2.2	499
4	NANOG-dependent function of TET1 and TET2 in establishment of pluripotency. Nature, 2013, 495, 370-374.	13.7	376
5	Competitive adsorption of Pb(II), Cu(II) and Zn(II) onto xanthate-modified magnetic chitosan. Journal of Hazardous Materials, 2012, 221-222, 155-161.	6.5	364
6	The simultaneous detection and removal of organophosphorus pesticides by a novel Zr-MOF based smart adsorbent. Journal of Materials Chemistry A, 2018, 6, 2184-2192.	5.2	214
7	Amino-Functionalized Al–MOF for Fluorescent Detection of Tetracyclines in Milk. Journal of Agricultural and Food Chemistry, 2019, 67, 1277-1283.	2.4	208
8	One-pot synthesis of multifunctional magnetic ferrite–MoS ₂ –carbon dot nanohybrid adsorbent for efficient Pb(<scp>ii</scp>) removal. Journal of Materials Chemistry A, 2016, 4, 3893-3900.	5.2	205
9	A self-standing nanoporous MoP ₂ nanosheet array: an advanced pH-universal catalytic electrode for the hydrogen evolution reaction. Journal of Materials Chemistry A, 2016, 4, 7169-7173.	5.2	204
10	Oxygenâ€Generating MnO ₂ Nanodotsâ€Anchored Versatile Nanoplatform for Combined Chemoâ€Photodynamic Therapy in Hypoxic Cancer. Advanced Functional Materials, 2018, 28, 1706375.	7.8	203
11	Interface engineering of metal organic framework on graphene oxide with enhanced adsorption capacity for organophosphorus pesticide. Chemical Engineering Journal, 2017, 313, 19-26.	6.6	190
12	Wet-chemistry topotactic synthesis of bimetallic iron–nickel sulfide nanoarrays: an advanced and versatile catalyst for energy efficient overall water and urea electrolysis. Journal of Materials Chemistry A, 2018, 6, 4346-4353.	5.2	181
13	Mechanism insight into rapid photocatalytic disinfection of Salmonella based on vanadate QDs-interspersed g-C3N4 heterostructures. Applied Catalysis B: Environmental, 2018, 225, 228-237.	10.8	165
14	Traditional NiCo ₂ S ₄ Phase with Porous Nanosheets Array Topology on Carbon Cloth: A Flexible, Versatile and Fabulous Electrocatalyst for Overall Water and Urea Electrolysis. ACS Sustainable Chemistry and Engineering, 2018, 6, 5011-5020.	3.2	164
15	Dynamic epigenomic landscapes during early lineage specification in mouse embryos. Nature Genetics, 2018, 50, 96-105.	9.4	164
16	Internally extended growth of core–shell NH ₂ -MIL-101(Al)@ZIF-8 nanoflowers for the simultaneous detection and removal of Cu(<scp>ii</scp>). Journal of Materials Chemistry A, 2018, 6, 21029-21038.	5.2	150
17	High effective adsorption/removal of illegal food dyes from contaminated aqueous solution by Zr-MOFs (UiO-67). Food Chemistry, 2018, 254, 241-248.	4.2	142
18	NH ₂ -MIL-53(Al) Metal–Organic Framework as the Smart Platform for Simultaneous High-Performance Detection and Removal of Hg ²⁺ . Inorganic Chemistry, 2019, 58, 12573-12581.	1.9	128

#	Article	IF	CITATIONS
19	A practical-oriented NiFe-based water-oxidation catalyst enabled by ambient redox and hydrolysis co-precipitation strategy. Applied Catalysis B: Environmental, 2019, 244, 844-852.	10.8	125
20	RNA-dependent chromatin targeting of TET2 for endogenous retrovirus control in pluripotent stem cells. Nature Genetics, 2018, 50, 443-451.	9.4	122
21	A colorimetric paper sensor based on the domino reaction of acetylcholinesterase and degradable γ-MnOOH nanozyme for sensitive detection of organophosphorus pesticides. Sensors and Actuators B: Chemical, 2019, 290, 573-580.	4.0	122
22	Shapeable three-dimensional CMC aerogels decorated with Ni/Co-MOF for rapid and highly efficient tetracycline hydrochloride removal. Chemical Engineering Journal, 2019, 375, 122076.	6.6	118
23	Amorphous Fe/Mn bimetal–organic frameworks: outer and inner structural designs for efficient arsenic(<scp>iii</scp>) removal. Journal of Materials Chemistry A, 2019, 7, 2845-2854.	5.2	118
24	Portable Colorimetric Detection of Mercury(II) Based on a Non-Noble Metal Nanozyme with Tunable Activity. Inorganic Chemistry, 2019, 58, 1638-1646.	1.9	118
25	Versatile molybdenum disulfide based antibacterial composites for in vitro enhanced sterilization and in vivo focal infection therapy. Nanoscale, 2016, 8, 11642-11648.	2.8	117
26	A one-step approach to the large-scale synthesis of functionalized MoS ₂ nanosheets by ionic liquid assisted grinding. Nanoscale, 2015, 7, 10210-10217.	2.8	115
27	Template-free preparation of layer-stacked hierarchical porous carbons from coal tar pitch for high performance all-solid-state supercapacitors. Journal of Materials Chemistry A, 2017, 5, 15869-15878.	5.2	107
28	Oxidative Desulfurization of Dibenzothiophene Using Ozone and Hydrogen Peroxide in Ionic Liquid. Energy & Fuels, 2010, 24, 2527-2529.	2.5	106
29	Fluorometric determination of the antibiotic kanamycin by aptamer-induced FRET quenching and recovery between MoS2 nanosheets and carbon dots. Mikrochimica Acta, 2017, 184, 203-210.	2.5	102
30	Facile fabrication of robust MOF membranes on cloth via a CMC macromolecule bridge for highly efficient Pb(II) removal. Chemical Engineering Journal, 2018, 339, 230-239.	6.6	102
31	Au Promoted Nickel–Iron Layered Double Hydroxide Nanoarrays: A Modular Catalyst Enabling High-Performance Oxygen Evolution. ACS Applied Materials & Interfaces, 2017, 9, 19807-19814.	4.0	101
32	Conductive Leaflike Cobalt Metal–Organic Framework Nanoarray on Carbon Cloth as a Flexible and Versatile Anode toward Both Electrocatalytic Glucose and Water Oxidation. Inorganic Chemistry, 2018, 57, 8422-8428.	1.9	99
33	Influence of metal ionic characteristics on their biosorption capacity by Saccharomyces cerevisiae. Applied Microbiology and Biotechnology, 2007, 74, 911-917.	1.7	97
34	Copper metal–organic frameworks loaded on chitosan film for the efficient inhibition of bacteria and local infection therapy. Nanoscale, 2019, 11, 11830-11838.	2.8	97
35	Preparation and electrochemical performance of the layered cobalt oxide (Co3O4) as supercapacitor electrode material. Journal of Solid State Electrochemistry, 2013, 17, 55-61.	1.2	96
36	Layered vanadium(IV) disulfide nanosheets as a peroxidase-like nanozyme for colorimetric detection of glucose. Mikrochimica Acta, 2018, 185, 7.	2.5	96

#	Article	IF	CITATIONS
37	One-pot synthesis of NiFe2O4 integrated with EDTA-derived carbon dots for enhanced removal of tetracycline. Chemical Engineering Journal, 2017, 310, 187-196.	6.6	92
38	Zfp281 Coordinates Opposing Functions of Tet1 and Tet2 in Pluripotent States. Cell Stem Cell, 2016, 19, 355-369.	5.2	89
39	Mixed-Valence Ce-BPyDC Metal–Organic Framework with Dual Enzyme-like Activities for Colorimetric Biosensing. Inorganic Chemistry, 2019, 58, 11382-11388.	1.9	89
40	Ultra technically-simple and sensitive detection for Salmonella Enteritidis by immunochromatographic assay based on gold growth. Food Control, 2018, 84, 536-543.	2.8	87
41	Highly sensitive furazolidone monitoring in milk by a signal amplified lateral flow assay based on magnetite nanoparticles labeled dual-probe. Food Chemistry, 2018, 261, 131-138.	4.2	82
42	Bioinspired foam with large 3D macropores for efficient solar steam generation. Journal of Materials Chemistry A, 2018, 6, 16220-16227.	5.2	81
43	ssDNA-tailorable oxidase-mimicking activity of spinel MnCo2O4 for sensitive biomolecular detection in food sample. Sensors and Actuators B: Chemical, 2018, 269, 79-87.	4.0	75
44	Rational construction of a robust metal-organic framework nanozyme with dual-metal active sites for colorimetric detection of organophosphorus pesticides. Journal of Hazardous Materials, 2022, 423, 127253.	6.5	75
45	Prussian blue nanoparticles based lateral flow assay for high sensitive determination of clenbuterol. Sensors and Actuators B: Chemical, 2018, 275, 223-229.	4.0	74
46	Label-free strip sensor based on surface positively charged nitrogen-rich carbon nanoparticles for rapid detection of Salmonella enteritidis. Biosensors and Bioelectronics, 2019, 132, 360-367.	5.3	74
47	The highly efficient elimination of intracellular bacteria <i>via</i> a metal organic framework (MOF)-based three-in-one delivery system. Nanoscale, 2019, 11, 9468-9477.	2.8	71
48	Patulin removal from apple juice using a novel cysteine-functionalized metal-organic framework adsorbent. Food Chemistry, 2019, 270, 1-9.	4.2	70
49	Highly Sensitive Colorimetric/Surface-Enhanced Raman Spectroscopy Immunoassay Relying on a Metallic Core–Shell Au/Au Nanostar with Clenbuterol as a Target Analyte. Analytical Chemistry, 2021, 93, 8362-8369.	3.2	70
50	Facet-selective response of trigger molecule to CeO2 {1 1 0} for up-regulating oxidase-like activity. Chemical Engineering Journal, 2017, 330, 746-752.	6.6	69
51	One-pot bottom-up fabrication of a 2D/2D heterojuncted nanozyme towards optimized peroxidase-like activity for sulfide ions sensing. Sensors and Actuators B: Chemical, 2020, 306, 127565.	4.0	69
52	Rapid fabrication of wearable carbon nanotube/graphite strain sensor for real-time monitoring of plant growth. Carbon, 2019, 147, 295-302.	5.4	68
53	CO ₂ Capture with Activated Carbon Grafted by Nitrogenous Functional Groups. Energy & Fuels, 2013, 27, 4818-4823.	2.5	67
54	Tet Enzymes Regulate Telomere Maintenance and Chromosomal Stability of Mouse ESCs. Cell Reports, 2016, 15, 1809-1821.	2.9	67

#	Article	IF	CITATIONS
55	Surface engineering of hierarchical Ni(OH)2 nanosheet@nanowire configuration toward superior urea electrolysis. Electrochimica Acta, 2018, 268, 211-217.	2.6	67
56	Insights into rapid photodynamic inactivation mechanism of Staphylococcus aureus via rational design of multifunctional nitrogen-rich carbon-coated bismuth/cobalt nanoparticles. Applied Catalysis B: Environmental, 2019, 241, 167-177.	10.8	67
57	Nanozyme amplification mediated on-demand multiplex lateral flow immunoassay with dual-readout and broadened detection range. Biosensors and Bioelectronics, 2020, 169, 112610.	5.3	67
58	Enhanced visible-light-driven photocatalytic sterilization of tungsten trioxide by surface-engineering oxygen vacancy and carbon matrix. Chemical Engineering Journal, 2018, 348, 292-300.	6.6	66
59	In-Situ Fixation of All-Inorganic Mo–Fe–S Clusters for the Highly Selective Removal of Lead(II). ACS Applied Materials & Interfaces, 2017, 9, 32720-32726.	4.0	65
60	Surface Engineering of Carbon Fiber Paper toward Exceptionally High-Performance and Stable Electrochemical Nitrite Sensing. ACS Sensors, 2019, 4, 2980-2987.	4.0	63
61	Functional nanozyme mediated multi-readout and label-free lateral flow immunoassay for rapid detection of Escherichia coli O157:H7. Food Chemistry, 2020, 329, 127224.	4.2	63
62	Dual recognition strategy and magnetic enrichment based lateral flow assay toward Salmonella enteritidis detection. Talanta, 2020, 206, 120204.	2.9	62
63	Graphitic carbon nitride (g-C3N4)-based nanostructured materials for photodynamic inactivation: Synthesis, efficacy and mechanism. Chemical Engineering Journal, 2021, 404, 126528.	6.6	61
64	Agar Aerogel Containing Small-Sized Zeolitic Imidazolate Framework Loaded Carbon Nitride: A Solar-Triggered Regenerable Decontaminant for Convenient and Enhanced Water Purification. ACS Sustainable Chemistry and Engineering, 2017, 5, 9347-9354.	3.2	60
65	Rational Surface Tailoring Oxygen Functional Groups on Carbon Spheres for Capacitive Mechanistic Study. ACS Applied Materials & amp; Interfaces, 2019, 11, 13214-13224.	4.0	58
66	A hybrid monolithic column based on layered double hydroxide-alginate hydrogel for selective solid phase extraction of lead ions in food and water samples. Food Chemistry, 2018, 257, 155-162.	4.2	57
67	Nitrogen and sulfur Co-doped microporous activated carbon macro-spheres for CO2 capture. Journal of Colloid and Interface Science, 2018, 526, 174-183.	5.0	56
68	Deep Catalytic Oxidative Desulfurization of Model Fuel Based on Modified Iron Porphyrins in Ionic Liquids: Anionic Ligand Effect. ACS Sustainable Chemistry and Engineering, 2017, 5, 2050-2055.	3.2	55
69	Polydopamine nanospheres as high-affinity signal tag towards lateral flow immunoassay for sensitive furazolidone detection. Food Chemistry, 2020, 315, 126310.	4.2	54
70	Bacterial capture efficiency in fluid bloodstream improved by bendable nanowires. Nature Communications, 2018, 9, 444.	5.8	53
71	An innovative immunochromatography assay for highly sensitive detection of 17β-estradiol based on an indirect probe strategy. Sensors and Actuators B: Chemical, 2019, 289, 48-55.	4.0	53
72	Surface Engineering of a Nickel Oxide–Nickel Hybrid Nanoarray as a Versatile Catalyst for Both Superior Water and Urea Oxidation. Inorganic Chemistry, 2018, 57, 4693-4698.	1.9	51

#	Article	IF	CITATIONS
73	Energy-efficient 1.67ÂV single- and 0.90 V dual-electrolyte based overall water-electrolysis devices enabled by a ZIF-L derived acid–base bifunctional cobalt phosphide nanoarray. Journal of Materials Chemistry A, 2018, 6, 24277-24284.	5.2	51
74	Template-Free Synthesis of Honeycomblike Porous Carbon Rich in Specific 2–5 nm Mesopores from a Pitch-Based Polymer for a High-Performance Supercapacitor. ACS Sustainable Chemistry and Engineering, 2019, 7, 2116-2126.	3.2	51
75	Enhanced functional properties of chitosan films incorporated with curcumin-loaded hollow graphitic carbon nitride nanoparticles for bananas preservation. Food Chemistry, 2022, 366, 130539.	4.2	51
76	Fluorometric determination of dopamine by using molybdenum disulfide quantum dots. Mikrochimica Acta, 2018, 185, 234.	2.5	50
77	Polybenzoxazine-based nitrogen-containing porous carbons for high-performance supercapacitor electrodes and carbon dioxide capture. RSC Advances, 2015, 5, 5331-5342.	1.7	49
78	An improved clenbuterol detection by immunochromatographic assay with bacteria@Au composite as signal amplifier. Food Chemistry, 2018, 262, 48-55.	4.2	49
79	Development of a specific nanobody and its application in rapid and selective determination of Salmonella enteritidis in milk. Food Chemistry, 2020, 310, 125942.	4.2	48
80	The roles of TET family proteins in development and stem cells. Development (Cambridge), 2020, 147, .	1.2	48
81	An Integrating Platform of Ratiometric Fluorescent Adsorbent for Unconventional Real-Time Removing and Monitoring of Copper Ions. ACS Applied Materials & Interfaces, 2020, 12, 13189-13199.	4.0	46
82	Highly Sensitive and Selective Determination of Tertiary Butylhydroquinone in Edible Oils by Competitive Reaction Induced "On–Off–On―Fluorescent Switch. Journal of Agricultural and Food Chemistry, 2016, 64, 706-713.	2.4	45
83	Adsorptive catalysis of hierarchical porous heteroatom-doped biomass: from recovered heavy metal to efficient pollutant decontamination. Journal of Materials Chemistry A, 2018, 6, 16690-16698.	5.2	45
84	lonic silver-infused peroxidase-like metal–organic frameworks as versatile "antibiotic―for enhanced bacterial elimination. Nanoscale, 2020, 12, 16330-16338.	2.8	45
85	Monolithic copper selenide submicron particulate film/copper foam anode catalyst for ultrasensitive electrochemical glucose sensing in human blood serum. Journal of Materials Chemistry B, 2018, 6, 718-724.	2.9	44
86	A photothermal and self-induced Fenton dual-modal antibacterial platform for synergistic enhanced bacterial elimination. Applied Catalysis B: Environmental, 2021, 295, 120315.	10.8	43
87	In-situ synthesis of self-standing cobalt-doped nickel sulfide nanoarray as a recyclable and integrated catalyst for peroxymonosulfate activation. Applied Catalysis B: Environmental, 2022, 307, 121184.	10.8	43
88	Self-ZIF template-directed synthesis of a CoS nanoflake array as a Janus electrocatalyst for overall water splitting. Inorganic Chemistry Frontiers, 2019, 6, 2090-2095.	3.0	42
89	Applicability of biological dye tracer in strip biosensor for ultrasensitive detection of pathogenic bacteria. Food Chemistry, 2019, 274, 816-821.	4.2	42
90	Selective removal of heavy metal ions in aqueous solutions by sulfide-selector intercalated layered double hydroxide adsorbent. Journal of Materials Science and Technology, 2019, 35, 1809-1816.	5.6	41

#	Article	IF	CITATIONS
91	Surface engineering of nickel selenide nanosheets array on nickel foam: An integrated anode for glucose sensing. Sensors and Actuators B: Chemical, 2019, 278, 110-116.	4.0	41
92	Oxygen-rich hierarchically porous carbons derived from pitch-based oxidized spheres for boosting the supercapacitive performance. Journal of Colloid and Interface Science, 2019, 540, 439-447.	5.0	39
93	A signal-on fluorescent sensor for ultra-trace detection of Hg2+ via Ag+ mediated sulfhydryl functionalized carbon dots. Carbon, 2019, 149, 355-363.	5.4	39
94	Dual-signal based immunoassay for colorimetric and photothermal detection of furazolidone. Sensors and Actuators B: Chemical, 2021, 331, 129431.	4.0	39
95	Luminescent metal-organic frameworks (LMOFs): An emerging sensing platform for food quality and safety control. Trends in Food Science and Technology, 2021, 111, 716-730.	7.8	39
96	Rational design of smart adsorbent equipped with a sensitive indicator via ligand exchange: A hierarchical porous mixed-ligand MOF for simultaneous removal and detection of Hg2+. Nano Research, 2021, 14, 1523-1532.	5.8	38
97	Photothermal-boosted effect of binary Cu Fe bimetallic magnetic MOF heterojunction for high-performance photo-Fenton degradation of organic pollutants. Science of the Total Environment, 2021, 795, 148883.	3.9	38
98	DNA-mediated gold nanoparticle signal transducers for combinatorial logic operations and heavy metal ions sensing. Biosensors and Bioelectronics, 2015, 72, 218-224.	5.3	37
99	Thiocholine-triggered reaction in personal glucose meters for portable quantitative detection of organophosphorus pesticide. Analytica Chimica Acta, 2019, 1060, 97-102.	2.6	37
100	In Situ Cascade Derivation toward a Hierarchical Layered Double Hydroxide Magnetic Absorbent for High-Performance Protein Separation. ACS Sustainable Chemistry and Engineering, 2020, 8, 4966-4974.	3.2	37
101	New Functional Tracer—Two-Dimensional Nanosheet-Based Immunochromatographic Assay for <i>Salmonella enteritidis</i> Detection. Journal of Agricultural and Food Chemistry, 2019, 67, 6642-6649.	2.4	36
102	Copper-Sensitized "Turn On―Peroxidase-Like Activity of MMoO ₄ (M = Co, Ni) Flowers for Selective Detection of Aquatic Copper Ions. ACS Sustainable Chemistry and Engineering, 2020, 8, 12568-12576.	3.2	36
103	Dextran-stabilized Fe-Mn bimetallic oxidase-like nanozyme for total antioxidant capacity assay of fruit and vegetable food. Food Chemistry, 2022, 371, 131115.	4.2	36
104	Ultrasensitive label-free immunochromatographic strip sensor for Salmonella determination based on salt-induced aggregated gold nanoparticles. Food Chemistry, 2021, 343, 128518.	4.2	35
105	Antibiotic-loaded MoS ₂ nanosheets to combat bacterial resistance via biofilm inhibition. Nanotechnology, 2017, 28, 225101.	1.3	34
106	Chemical-staining based lateral flow immunoassay: A nanomaterials-free and ultra-simple tool for a small molecule detection. Sensors and Actuators B: Chemical, 2019, 279, 427-432.	4.0	34
107	Antibiotic and mammal IgG based lateral flow assay for simple and sensitive detection of Staphylococcus aureus. Food Chemistry, 2021, 339, 127955.	4.2	34
108	Engineering multi-stage nickel oxide rod-on-sheet nanoarrays on Ni foam: A superior catalytic electrode for ultrahigh-performance electrochemical sensing of glucos. Sensors and Actuators B: Chemical, 2018, 255, 416-423.	4.0	33

#	Article	IF	CITATIONS
109	Visible light responsive, self-activated bionanocomposite films with sustained antimicrobial activity for food packaging. Food Chemistry, 2021, 362, 130201.	4.2	33
110	Conductive polyaniline-graphene oxide sorbent for electrochemically assisted solid-phase extraction of lead ions in aqueous food samples. Analytica Chimica Acta, 2020, 1100, 57-65.	2.6	32
111	Nanobodies Based on a Sandwich Immunoassay for the Detection of Staphylococcal Enterotoxin B Free from Interference by Protein A. Journal of Agricultural and Food Chemistry, 2020, 68, 5959-5968.	2.4	32
112	Highly specific and sensitive determination of propyl gallate in food by a novel fluorescence sensor. Food Chemistry, 2018, 256, 45-52.	4.2	31
113	Microphase Separation Engineering toward 3D Porous Carbon Assembled from Nanosheets for Flexible All-Solid-State Supercapacitors. ACS Applied Materials & Interfaces, 2022, 14, 13250-13260.	4.0	31
114	Mussel-inspired Fe-based Tannic acid Nanozyme: A renewable bioresource-derived high-affinity signal tag for dual-readout multiplex lateral flow immunoassay. Chemical Engineering Journal, 2022, 446, 137382.	6.6	29
115	Ambient self-derivation of nickel-cobalt hydroxysulfide multistage nanoarray for high-performance electrochemical glucose sensing. Applied Surface Science, 2020, 505, 144636.	3.1	28
116	A portable dual-mode colorimetric platform for sensitive detection of Hg2+ based on NiSe2 with Hg2+-Activated oxidase-like activity. Biosensors and Bioelectronics, 2022, 215, 114519.	5.3	28
117	An advanced and universal method to high-efficiently deproteinize plant polysaccharides by dual-functional tannic acid-felll complex. Carbohydrate Polymers, 2019, 226, 115283.	5.1	27
118	Facile synthesis of hierarchical mesopore-rich activated carbon with excellent capacitive performance. Journal of Colloid and Interface Science, 2019, 546, 101-112.	5.0	27
119	Rapid and selective fluorometric determination of tannic acid using MoO3-x quantum dots. Mikrochimica Acta, 2019, 186, 247.	2.5	27
120	Nature-inspired nanozymes as signal markers for in-situ signal amplification strategy: A portable dual-colorimetric immunochromatographic analysis based on smartphone. Biosensors and Bioelectronics, 2022, 210, 114289.	5.3	27
121	From lamellar to hierarchical: overcoming the diffusion barriers of sulfide-intercalated layered double hydroxides for highly efficient water treatment. Journal of Materials Chemistry A, 2017, 5, 22506-22511.	5.2	26
122	Highly sensitive detection of a small molecule by a paired labels recognition system based lateral flow assay. Analytical and Bioanalytical Chemistry, 2018, 410, 3161-3170.	1.9	26
123	Nanostructured morphology control and phase transition of zeolitic imidazolate frameworks as an ultra-high performance adsorbent for water purification. Inorganic Chemistry Frontiers, 2019, 6, 2667-2674.	3.0	26
124	An ultrasensitive sandwich chemiluminescent enzyme immunoassay based on phage-mediated double-nanobody for detection of Salmonella Typhimurium in food. Sensors and Actuators B: Chemical, 2022, 352, 131058.	4.0	26
125	Surface Oxygen Functionalization of Carbon Cloth toward Enhanced Electrochemical Dopamine Sensing. ACS Sustainable Chemistry and Engineering, 2021, 9, 16063-16072.	3.2	26
126	Missing-linker engineering of Eu (III)-doped UiO-MOF for enhanced detection of heavy metal ions. Chemical Engineering Journal, 2022, 431, 134050.	6.6	26

#	Article	IF	CITATIONS
127	Interfacial growth of nitrogen-doped carbon with multi-functional groups on the MoS2 skeleton for efficient Pb(II) removal. Science of the Total Environment, 2018, 631-632, 912-920.	3.9	25
128	Oxidase-like Fe–Mn bimetallic nanozymes for colorimetric detection of ascorbic acid in kiwi fruit. LWT - Food Science and Technology, 2022, 154, 112821.	2.5	25
129	Development of a streptavidin-bridged enhanced sandwich ELISA based on self-paired nanobodies for monitoring multiplex Salmonella serogroups. Analytica Chimica Acta, 2022, 1203, 339705.	2.6	25
130	Enhanced Exfoliation Effect of Solid Auxiliary Agent On the Synthesis of Biofunctionalized MoS ₂ Using Grindstone Chemistry. Particle and Particle Systems Characterization, 2016, 33, 825-832.	1.2	24
131	Strong coordination ability of sulfur with cobalt for facilitating scale-up synthesis of Co9S8 encapsulated S, N co-doped carbon as a trifunctional electrocatalyst for oxygen reduction reaction, oxygen and hydrogen evolution reaction. Journal of Colloid and Interface Science, 2022, 608, 2623-2632.	5.0	24
132	Mechanical penetration of β-lactam–resistant Gram-negative bacteria by programmable nanowires. Science Advances, 2020, 6, .	4.7	23
133	Graphite-like carbon nitride-laden gold nanoparticles as signal amplification label for highly sensitive lateral flow immunoassay of 17β-estradiol. Food Chemistry, 2021, 347, 129001.	4.2	23
134	Competitive Lateral Flow Immunoassay Relying on Au–SiO ₂ Janus Nanoparticles with an Asymmetric Structure and Function for Furazolidone Residue Monitoring. Journal of Agricultural and Food Chemistry, 2021, 69, 511-519.	2.4	23
135	Highly efficient and cost-effective removal of patulin from apple juice by surface engineering of diatomite with sulfur-functionalized graphene oxide. Food Chemistry, 2019, 300, 125111.	4.2	22
136	An integrated nanoflower-like MoS2@CuCo2O4 heterostructure for boosting electrochemical glucose sensing in beverage. Food Chemistry, 2022, 396, 133630.	4.2	22
137	Label-free fluorescence aptasensor for sensitive determination of bisphenol S by the salt-adjusted FRET between CQDs and MoS2. Sensors and Actuators B: Chemical, 2018, 259, 717-724.	4.0	21
138	Small size nanoparticles—Co3O4 based lateral flow immunoassay biosensor for highly sensitive and rapid detection of furazolidone. Talanta, 2020, 211, 120729.	2.9	21
139	Acid-Induced Self-Catalyzing Platform Based on Dextran-Coated Copper Peroxide Nanoaggregates for Biofilm Treatment. ACS Applied Materials & Interfaces, 2021, 13, 29269-29280.	4.0	21
140	Extractive and oxidative desulfurization of model oil in polyethylene glycol. RSC Advances, 2016, 6, 35071-35075.	1.7	20
141	Biomimetic cell model for fluorometric and smartphone colorimetric dual-signal readout detection of bacterial toxin. Sensors and Actuators B: Chemical, 2020, 312, 127956.	4.0	20
142	Bioresource-derived tannic acid-supported immuno-network in lateral flow immunoassay for sensitive clenbuterol monitoring. Food Chemistry, 2022, 382, 132390.	4.2	20
143	One-pot extractive and oxidative desulfurization of liquid fuels with molecular oxygen in ionic liquids. RSC Advances, 2014, 4, 59885-59889.	1.7	18
144	An environmentally friendly deproteinization and decolorization method for polysaccharides of Typha angustifolia based on a metal ion-chelating resin adsorption. Industrial Crops and Products, 2019, 134, 160-167.	2.5	18

#	Article	IF	CITATIONS
145	High-performance electrochemical nitrite sensing enabled using commercial carbon fiber cloth. Inorganic Chemistry Frontiers, 2019, 6, 1501-1506.	3.0	18
146	Developing a Simple Immunochromatography Assay for Clenbuterol with Sensitivity by One-Step Staining. Journal of Agricultural and Food Chemistry, 2020, 68, 15509-15515.	2.4	18
147	Controllable assembly metal-organic frameworks and gold nanoparticles composites for sensitive immunochromatographic assay. Food Chemistry, 2022, 367, 130737.	4.2	18
148	Facile construction of Fe3+/Fe2+ mediated charge transfer pathway in MIL-101 for effective tetracycline degradation. Journal of Cleaner Production, 2022, 359, 131808.	4.6	17
149	Aerogel doped by sulfur-functionalized graphene oxide with convenient separability for efficient patulin removal from apple juice. Food Chemistry, 2021, 338, 127785.	4.2	16
150	Lateral flow immunoassay for furazolidone point-of-care testing: Cater to the call of saving time, labor, and cost by coomassie brilliant blue labeling. Food Chemistry, 2021, 352, 129415.	4.2	16
151	An immune-scaffold relying biosensor for simultaneous detection of nitrofurazone and furazolidone. Sensors and Actuators B: Chemical, 2021, 345, 130399.	4.0	16
152	A facile and green synthesis of CDs-MoS2-Fe3O4 nanohybrid for recyclable and enhanced photocatalysis in dye degradation. Materials Letters, 2018, 232, 167-170.	1.3	15
153	Ultraâ€Deep Oxidative Desulfurization of Model Oil Catalyzed by In Situ Carbonâ€Supported Vanadium Oxides Using Cumene Hydroperoxide as Oxidant. ChemistrySelect, 2020, 5, 2148-2156.	0.7	15
154	A Conductive Network and Dipole Field for Harnessing Photogenerated Charge Kinetics. Advanced Materials, 2021, 33, e2104099.	11.1	15
155	Natural Sugar: A Green Assistance To Efficiently Exfoliate Inorganic Layered Nanomaterials. Inorganic Chemistry, 2018, 57, 5560-5566.	1.9	14
156	Immunoassay of clenbuterol with bacteria as natural signal carriers for signal amplification. Sensors and Actuators B: Chemical, 2019, 288, 210-216.	4.0	14
157	Demand-oriented construction of Mo3S13-LDH: A versatile scavenger for highly selective and efficient removal of toxic Ag(I), Hg(II), As(III), and Cr(VI) from water. Science of the Total Environment, 2022, 820, 153334.	3.9	14
158	Vanadium Disulfide Nanosheet Boosts Optical Signal Brightness as a Superior Enzyme Label to Improve the Sensitivity of Lateral Flow Immunoassay. Analytical Chemistry, 2022, 94, 8693-8703.	3.2	14
159	Biomass reinforced graphene oxide solid/liquid phase membrane extraction for the measurement of Pb(II) in food samples. Food Chemistry, 2018, 269, 9-15.	4.2	13
160	Self-Assembling Antibody Network Simplified Competitive Multiplex Lateral Flow Immunoassay for Point-of-Care Tests. Analytical Chemistry, 2022, 94, 1585-1593.	3.2	13
161	Multiplex immunochromatographic platform based on crystal violet tag for simultaneous detection of streptomycin and chloramphenicol. Food Chemistry, 2022, 393, 133351.	4.2	13
162	Preparation of spherical activated carbon with hierarchical porous texture. Journal of Materials Science, 2009, 44, 4750-4753.	1.7	12

#	Article	IF	CITATIONS
163	Hydrogel loading 2D montmorillonite exfoliated by anti-inflammatory Lycium barbarum L. polysaccharides for advanced wound dressing. International Journal of Biological Macromolecules, 2022, 209, 50-58.	3.6	12
164	Construction of In ₂ S ₃ @ZIF-8@ZnIn ₂ S ₄ hierarchical nanoflower heterostructures to promote photocatalytic reduction activity. Inorganic Chemistry Frontiers, 2021, 9, 51-59.	3.0	11
165	Carbon dots based multicolor fluorescence sensor for ratiometric and colorimetric dual-model detection of Cu2+. Dyes and Pigments, 2022, 203, 110381.	2.0	11
166	Mild resorcinol formaldehyde resin polymer based immunochromatography assay for high-sensitive detection of clenbuterol. Sensors and Actuators B: Chemical, 2021, 331, 129443.	4.0	10
167	Development of a Double Nanobody-Based Sandwich Immunoassay for the Detecting Staphylococcal Enterotoxin C in Dairy Products. Foods, 2021, 10, 2426.	1.9	10
168	White peroxidase-mimicking nanozymeË—nanocarrier of enzyme labeled antibody to enhance catalytic performance and relieve color interference of immunoassay. Sensors and Actuators B: Chemical, 2022, 364, 131909.	4.0	10
169	Energy-efficient electrolytic H2 production and high-value added H2-acid-base co-electrosynthesis modes enabled by a Ni2P catalyst in a diaphragm cell. Applied Catalysis B: Environmental, 2022, 317, 121726.	10.8	10
170	Effects of novolac resin modification on mechanical properties of carbon fiber/epoxy composites. Polymer Composites, 2011, 32, 227-235.	2.3	9
171	Does the intrinsic photocontrollable oxidase-mimicking activity of 2-aminoterephthalic acid dominate the activity of metal–organic frameworks?. Inorganic Chemistry Frontiers, 2021, 8, 3482-3490.	3.0	9
172	Natural Products Self-Assembled Nanozyme for Cascade Detection of Glucose and Bacterial Viability in Food. Foods, 2021, 10, 2596.	1.9	9
173	Gentiana straminea Maxim. polysaccharide decolored via high-throughput graphene-based column and its anti-inflammatory activity. International Journal of Biological Macromolecules, 2021, 193, 1727-1733.	3.6	8
174	Expanded detection range of lateral flow immunoassay endowed with a third-stage amplifier indirect probe. Food Chemistry, 2022, 377, 131920.	4.2	8
175	Emergence of dyestuff chemistry-encoded signal tracers in immunochromatographic assays: Fundamentals and recent food applications. Trends in Food Science and Technology, 2022, 127, 335-351.	7.8	8
176	Tetrathiomolybdate@ZIFs nanocrystal clusters: A novel modular and controllable catalyst for photocatalytic application. Materials and Design, 2019, 182, 108042.	3.3	7
177	Two-Dimensional Zeolitic Imidazolate Framework-L-Derived Iron–Cobalt Oxide Nanoparticle-Composed Nanosheet Array for Water Oxidation. Inorganic Chemistry, 2019, 58, 6231-6237.	1.9	7
178	A sustainable and nondestructive method to high-throughput decolor Lycium barbarum L. polysaccharides by graphene-based nano-decoloration. Food Chemistry, 2021, 338, 127749.	4.2	7
179	COVID-19-inspired "artificial virus―to combat drug-resistant bacteria by membrane-intercalation- photothermal-photodynamic multistage effects. Chemical Engineering Journal, 2022, 446, 137322.	6.6	7
180	Insights into high-efficient removal of tetracycline by a codoped mesoporous carbon adsorbent. Chinese Journal of Chemical Engineering, 2022, 44, 148-156.	1.7	6

#	Article	IF	CITATIONS
181	Neutral-Alkaline Hybrid Water Electrolysis at Less Than 1.43 V Enabled by a Branched NiCo-Hydroxysulfide Nanoarray. ACS Sustainable Chemistry and Engineering, 2021, 9, 15294-15302.	3.2	6
182	Lycium Barbarum Polysaccharide-Iron (III) Chelate as Peroxidase Mimics for Total Antioxidant Capacity Assay of Fruit and Vegetable Food. Foods, 2021, 10, 2800.	1.9	4
183	Bioinspired Neuron-like Adsorptive Networks for Heavy Metal Capture and Tunable Electrochemically Mediated Recovery. ACS Applied Materials & Interfaces, 2021, 13, 45077-45088.	4.0	3
184	Enriched sp ² -Hybridized C Atoms toward the Tradeoff between Activity, Conductivity and Stability of Spherical Porous Metal–Nitrogen–Carbon Catalysts for Rechargeable Zinc–Air Batteries. ACS Sustainable Chemistry and Engineering, 2022, 10, 9303-9314.	3.2	3
185	Physical and electrochemical characterization of activated carbons with high mesoporous ratio for supercapacitors based on ionic liquid as the electrolyte. Journal of Solid State Electrochemistry, 2011, 15, 607-613.	1.2	2
186	Asymmetric Electrolyte Design: Energy-Efficient Electrolytic Hydrogen Production under 0.95 V Driven by Janus Metal Phosphide Nanoarray. ACS Sustainable Chemistry and Engineering, 2021, 9, 16163-16171.	3.2	2
187	A multi-scenario dip-stick immunoassay of 17β-estradiol based on multifunctional and non-composite nanoparticles with colorimetric-nanozyme-magnetic properties. Sensors and Actuators B: Chemical, 2022, 367, 132150.	4.0	2
188	Experimental Investigation on the Propagation of Hydraulic Fractures through Coal-Rock Interfaces. Advances in Materials Science and Engineering, 2021, 2021, 1-14.	1.0	1
189	A one-pot synthesis of PEGylated plasmonic WO _{3â~'<i>x</i>} @Eugenol nanoflowers with NIR-controllable antioxidant activities for synergetically combating bacterial biofilm infection. Inorganic Chemistry Frontiers, 2022, 9, 3808-3819.	3.0	1